25th IMEKO TC4 International Symposium
23rd International Workshop on ADC and DAC Modelling and Testing
IMEKO TC-4 2020
Brescia, Italy / September 12-14, 2022

Lithium-Ion Batteries state of charge estimation based on electrochemical impedance spectroscopy and convolutional neural network

Emanuele Buchicchio[1], Alessio De Angelis[1], Francesco Santoni[1], Paolo Carbone[1]

[1]*Department of Engineering University of Perugia, Via G. Duranti, 93 - 06125 - PERUGIA, emanuele.buchicchio@studenti.unipg.it, alessio.deangelis@unipg.it, francesco.santoni@unipg.it, paolo.carbone@unipg.it*

***Abstract* – Estimating the state of charge of batteries is a critical task for every battery-powered device. In this work, we propose a machine learning approach based on electrochemical impedance spectroscopy and convolutional neural networks. A case study based on Samsung ICR18650-26J lithium-Ion batteries is also presented and discussed in detail. A classification accuracy of 80% and top-2 classification accuracy of 95% were achieved on a test battery not used for model training.**

I. INTRODUCTION

Many battery-powered devices such as laptops, smartphones, cameras, tablets, cordless shavers, lawnmowers, drones, and even electric cars are now part of our daily life. In most battery-operated systems, knowing the remaining charge within the battery is essential for end-users. In addition, the knowledge of the remaining battery capacity is fundamental for its management because states of extremely high or extremely low state-of-charge (SOC) can irreversibly damage the battery [1]. The relationship between the battery's observable signals and the estimated SOC is highly non-linear, varying with temperature and discharge/charge currents [2].

There is no practical method for SOC direct measurement outside laboratory settings [3]. Therefore, many research works have been conducted over the last decades to develop a secure, practical, and reliable method for SOC estimation [4, 5].

The data-driven SOC estimation approaches require limited knowledge about internal battery characteristics. In contrast, model-driven approaches require an in-depth understanding of the battery's internal chemical ed electrical characteristics. Model-based methods also require the assumption that the battery model is accurately established. This condition is hard to realize in real applications due to the effect of measurement noise and model parameter drifts with aging, and temperature [3]. Combining some a-priori information, embedded in physical electrochemical models or electrical equivalent circuit models, with experimental data, model-based approach can result in reliable and accurate predictions [6]. However, they require extensive domain knowledge and relatively long development times. Common model-based approaches in recent publications include the usage of Sliding Mode Observer, Luenberger Observer, Kalman filters, Electrochemical Model, Equivalent Circuit Model, Electrochemical Impedance Model [7].

Data-driven approaches, such as those based on machine learning (ML), are becoming more popular for estimating the SOC and battery state-of-health (SOH) due to the greater availability of battery data and improved computing power capabilities. SOC estimators based on neural networks (NN) have been studied extensively in the literature. When using the NN model, a large amount of known input data and expected output data obtained from the battery charging and discharging experiments is required to train the network and extract the fitting relationship without an a-priori model of the battery.

Traditional ML techniques contain no more than one or two layers of non-linear and linear transformations. With the advent of faster computational power and an abundance of available real-world data, more complex architectures were investigated, which, in many cases, allowed researchers to make striking improvements in many applications. The deep learning architecture used in this work, called a deep residual network, won the 2015 ImageNet challenge with an error rate of 3.57% which even surpasses human-level accuracy valued at 5.1% [8] for the same task.

II. MATERIALS AND METHODS

A. *SoC estimation using Electrochemical impedance spectroscopy and Convolutional Neural Networks*

Electrochemical impedance spectroscopy (EIS) is a powerful tool for monitoring SOC and SOH of rechargeable batteries [9]. It provides an estimate of the equivalent battery impedance $Z(f)$ by, e.g., measuring the voltage variations at the battery contacts after a varying input current is applied. Visual representation of the results is often obtained by plotting the negative imaginary part of $Z(f)$ vs its real part.

Although it is easy to observe that different SOC values generate different shapes in EIS visual representations, the relationships between SOC and $Z(f)$ are not obvious. This

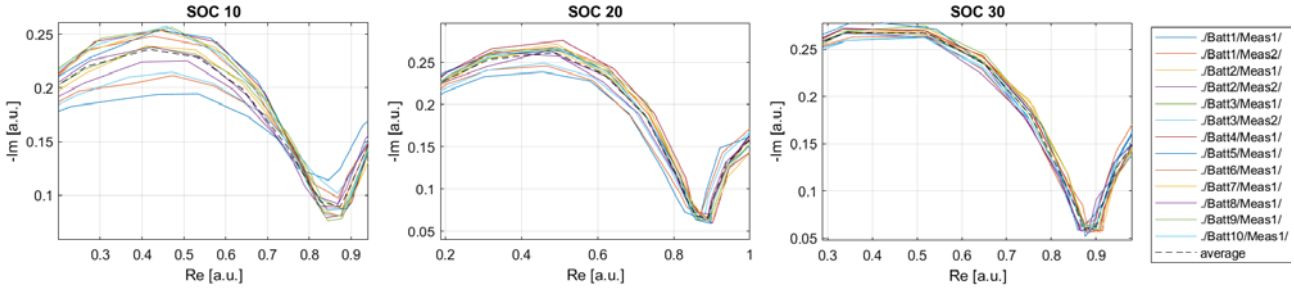

Fig. 1. Normalized EIS curve comparison. The shape of the curve is specific for each SOC internal state

is shown in figure 1 that is based on measurements of the $Z(f)$ of ten rechargeable batteries, characterized by three different SOCs.

Finding a closed-form derivation of this relationship appears an unfeasible task. However, we can approximate this unknown function by extracting information from experimental results. We can easily spot some differences in the visual representation of experimental data from different SOC conditions. EIS curves measured at the same SOC level show similar shape patterns, but exhibit translations in the complex plane. The magnitude of the translation varies for different batteries and even for the same battery across different measurements (figure 2). Using an ML-based approach to relate SOC to EIS-derived data requires the assumption that the EIS shape patterns depend on SOC and are invariant given the same battery type.

Convolutional Neural Networks (CNN) provide the three primary advantages for image processing [10] over the traditional feed-forward neural network with fully connected layers. Firstly, they have sparse connections instead of fully connected connections, which lead to reduced parameters and allow for processing high-dimensional data. Secondly, weight sharing across the entire image reduce memory requirements and causes translational equivariance property. Thirdly pooling layer bring invariance to the local translation property. The invariance and equivariance properties make CNN an ideal candidate for performing classification tasks on EIS curves such as those graphed in figure 2. Given that deep CNNs are the de-facto industry standard solution for image classification tasks, with many well-known architectures and pre-trained models available, we developed a CNN-based SOC estimator for EIS curves visual representation images.

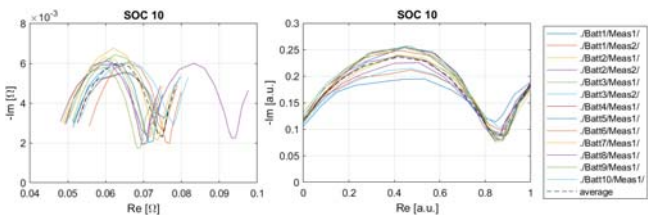

Fig. 2. Comparison of measured EIS curves at SOC 10%. *Original data (on the left) and normalized (on the right). EIS curves are similar in shape, but are translated. In one case, the translation is much more relevant*

B. Electrochemical impedance spectroscopy data acquisition

We are using a Keysight U2351A data acquisition board to provide the excitation signal by means of a 16-bit digital to analog converter (DAC) and to acquire the current and voltage signals by means of two 16-bit analog to digital converter (ADC) channels. The excitation signal is a random-phase multisine, i.e. the sum of harmonically-related sinusoids [11] that allows to simultaneously excite the battery at a wide range of frequencies. In this case, the excited frequencies are 0.05, 0.1, 0.2, 0.4, 1, 2, 4, 10, 20, 40, 100, 200, 400, and 1000 Hz in all measurements. The excitation signal generated by the DAC is converted to a current signal by a voltage-to-current converter custom circuit [12]. The current signal is measured across a known shunt resistor. The voltage signal across the battery is also measured by a second INA connected to the second ADC channel. The current and voltage signals acquired by the ADC channels are transferred to a PC to compute the discrete Fourier Transform (DFT) and calculate the complex impedance value at each excited frequency. The current amplitude at each excited frequency was 50 mA, which resulted in a measurement uncertainty of approximately 0.1 mΩ, as characterized in [13].

C. SOC estimation as a machine learning classification task

In machine learning, *classification* is the task of predicting the class to which an object belongs. Each object is uniquely represented by a set of values $x1, x2, \ldots, xl$, known as *features* in ML jargon. The l feature values, stacked together, in the common ML notation are labeled as the *feature vector* $x \in R^l$. The goal is to design a classifier $f(x)$, so that given a values in a feature vector x we will be able to predict the class of witch the object belong. To formulate the task in mathematical terms, each class is

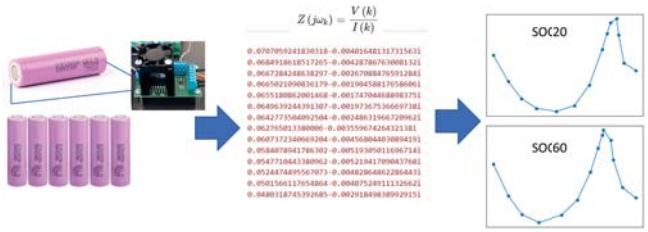

Fig. 3. EIS of battery is measured at different SOC using the system presented in [13]. The complex impedance values are then encoded in 2D visual representation to feed the convolutional neural network.

represented by the class label variable y and $\hat{y}$ denotes the predicted class given the value of x and the set of possible predicted classes in the so-called *vocabulary*:

$$\hat{y} = \Phi(f(x)), \tag{1}$$

where $\Phi(\cdot)$ is a nonlinear function that maps any possible $f(x)$ values to one on the class labels.

The set of possible SOC class *vocabulary* considered in this work is 100%, 90%, 80%, 70%, 60%, 50%, 40%, 30%, 20%, and 10%.

The raw features vectors is made by complex impedance values measured at frequencies $[0.05, 0.1, 0.2, 0.4, 1, 2, 4, 10, 20, 40, 100, 200, 400, 1000]$ Hz for a specific SOC. A two-dimensional visual representation of the impedance curve in the complex plane is used to build a 2D feature vector for each measured EIS (Figure 3).

D. Training and test dataset

We compiled and published two open-access dataset [14],[15] of data obtained through EIS, by measuring ten brand new Samsung ICR18650-26J lithium-Ion batteries at different SOCs. A detailed description of the measurement system is available in [13].

Two sets of EIS measurements have been kept out from training and validation as a test dataset for the final system performance assessment. These two test cases are representative of two different scenarios: 1) a new set of EIS data on battery that was originally included in model training; 2) A set of EIS originating from a battery never seen by the model during training and validation.

For the *new battery* test case we randomly choose one of the ten batteries. Battery 10 was among data in [14] and battery 06 among data in [15] For the *new measurement* test case we randomly choose a set of EIS from one measurement cycle. Measurement 10 on battery 01 was selected among data in [14] and measurement 8 on battery 05 among data in [15]

E. Training and validation workflow

We have developed a fully automated pipeline for training deep learning-based classifiers using the open-source libraries PyTorch and FastAI [16]. The workflow consists of three steps (Figure 4):

1. Step 1: data acquisition;
2. Step 2: data selection;
3. Step 3: model training.

The *Data acquisition* step produces a CSV file containing EIS spectra at each SOC. In *Data selection* the available data are split in training ad test datasets. The test dataset will only be used for test and not for training. The training dataset will be further split to hold out 20% data for validation. We implemented different training strategy for the *model training step*. In this work, we performed two different experiments adopting the *validation hold* strategy for the first one and the *leave k-out cross validation* strategy for the second one. In the *validation hold* experiment we trained a single model using 80% of the available data, while 20% of the data was set aside and used exclusively for validation. The performance of the model was then verified using the test dataset containing completely new measurements. In the second experiment we implemented the *leave k-out* strategy as *leave one battery out* to investigate the model performance dependency from a particular choice of training data-set and effects of specific battery inclusion in the training process. We run ten training sessions excluding data related to one of the batteries each time. This experiment produced ten trained models that can be used alone or combined in an *ensemble model* for SOC inference.

We published all the algorithms developed for this work in the open-source python *ML Measurement library* [17]. We also created several Jupyter notebooks with the high-level experiment workflow orchestration script executable on free *Google Colab* machine learning compute platform for easy experiment repeatability. The notebooks take advantage of the free Google Drive private storage associated with the user's account to store all trained models and generated images. While paid service subscriptions include more computational resources, the hardware and software configuration available with the free service allows running all experiments from scratch within a few hours. The notebook itself provides the installation of missing software components in the *setup* phase.

F. Efficient deep CNN training for SoC estimation

Many pre-trained deep learning models have proven adequate for image/video classification tasks. We chose the ResNet18 CNN because the residual network architecture achieves good results in image classification tasks and is

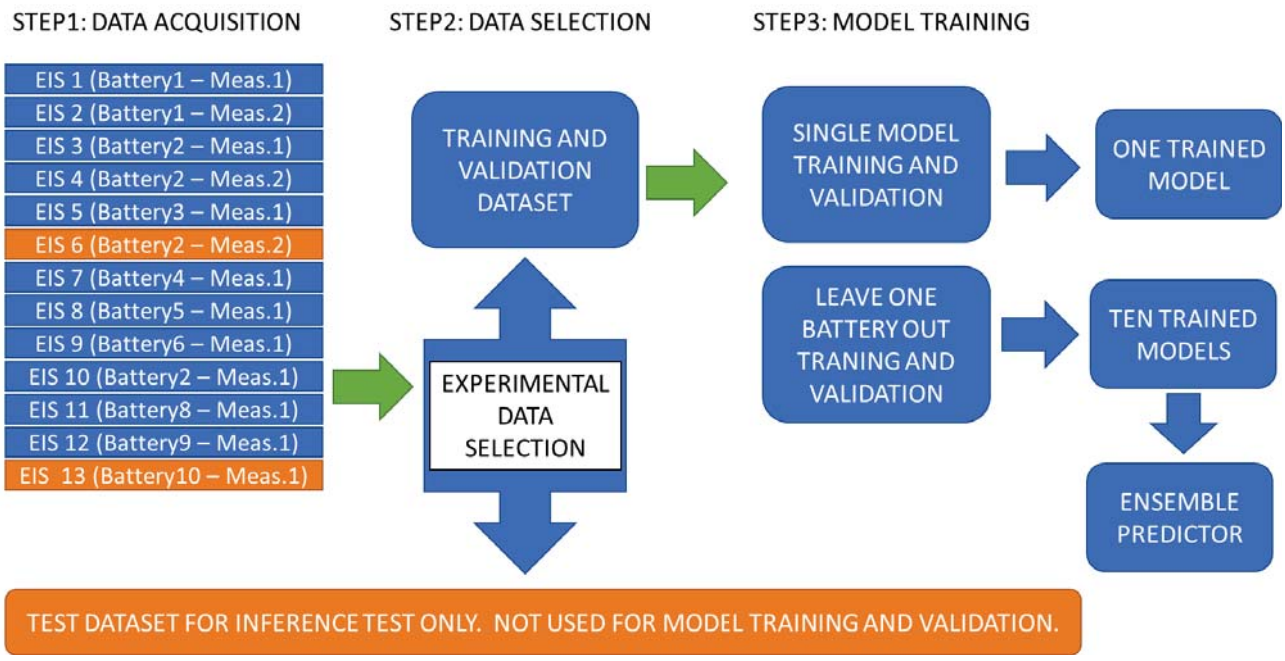

Fig. 4. SOC estimator training and validation workflow overview. The same workflow was applied to both dataset [14] and [15]

relatively fast to train [18]. Transfer learning from general-purpose image classification pre-trained models allows fast fine-tuning training of the deep CNN model. The optimal learning rate for training has been estimated with the Cyclical Learning Rates method [19] to avoid time-consuming multiple runs to perform hyper-parameters sweeps. The algorithm implementation in the FastAI library suggested a learning rate in the range $10^{-2} - 10^{-3}$. We perform the model fine-tuning with a sequence of freeze, fit-one-cycle, unfreeze, and fit-one-cycle operations using the *discriminative learning rate fine tuning* method developed in [20] and implemented in FastAI library [16].

After some tests, we set the training script to run for fifty epochs, although, in many case cases, few epochs would suffice.

G. Data Augmentation

For model training, we developed an *ad-hoc* data augmentation technique based on simulating additional measurements by adding white Gaussian noise within the uncertainty band estimated in [13]. The training pipeline generates for each available EIS spectrum K different visual representations with K equal to the augmentation factor parameter set in the experimental setup. The results shown in this article were obtained with $K = 10$.

H. System calibration

Experimental data revealed high variability across different batteries and also significant differences between measurements on the same battery at different times. For a field application, it is, therefore, necessary to tune the estimation model each time the battery is replaced and periodically to compensate for changes in the internal state of the battery that occur over time. This procedure can be performed as part of a periodic calibration procedure using hardware onboard the device or a dedicated external instrument that may be included in the docking station of the device. (e.g., in the charging station of an electric vehicle).

III. RESULTS

A. SOC curve analysis

Observing the visual representation of the EIS data resulting from the data pre-processing (Figure 3), we can see that are shape variations across different SOC for the same battery but also for the same SOC across different batteries (Figure 5).

B. Model validation

The SOC estimator model trained in the *validation hold* experiment achieves up to 100% accuracy score on the validation dataset. The accuracy depends on the amount of measurement noise used for data augmentation. Using a realistic amount of AWG noise according to the uncertainty band of the impedance measurement system estimated in [13], the model trained using data from the second dataset achieves an overall 87% accuracy The three models trained in the *leave one battery out* experiment achieved accuracy scores between 88% and 89%.

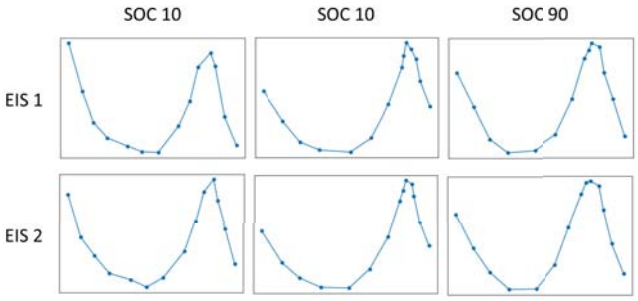

Fig. 5. EIS curves of two battery at SOC 10% *,* 30% *and* 90% *with differences across SOC for the same battery and across batteries for the same SOC.*

To verify that the SOC estimation produced is based on a reasonable set of image features, we compute the *class activation map* (CAM) [21] on some inference results using the implementation we published in [17]. CAMs allow to visually highlight the image areas that were more relevant to the final classification performed by a specific image classification neural network. The resulting heat map (Figure 6) shows that the main contributions to the SOC classification came from the peak and valley areas of the curves, whose shape changes with SOC.

C. Test in a SOC measurement system

We deploy the training model in an inference pipeline to simulate the usage in a real SOC estimation system. In a real application, the model training should be performed during the system calibration procedure to fine-tune the model on the actual battery that must be monitored. To evaluate the SOC estimator performance on realistic conditions we arrange two different test cases, representative of several use cases of the system:

1. New battery test: SOC estimation of a battery similar (same model) to the batteries used for model training but never connected to the system before.

2. New measure test: SOC estimation of one of the batteries used for training a few days after initial system calibration.

Model trained during both in *leave one battery out* and *validation hold* experiments was evaluated on the two test cases. In the real-world use of a battery system, an accurate estimate of SOC is often not necessary. In addition, impedance measurements are affected by several factors (such as temperature) that prevent accurate data from being obtained. Based on this consideration, k-accuracy in addition to accuracy, was used to evaluate the models. Multi-class classification metrics was computed using functions implemented of SciKit Learn [22] open-source library. The model trained in *validation hold* experiment

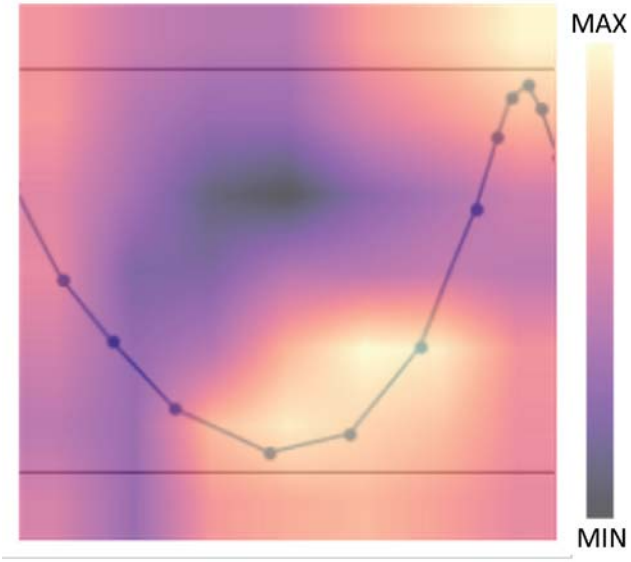

Fig. 6. Overlay of 7x7 class activation map on an EIS curve measured at SOC 40% *on battery 06. The brighter colors indicate a relative more significant contribution of feature (image pixels) in the area to the final classification.*

achieves 0.68 accuracy and 0.87 top2-accuracy on *new battery* test and 0.90 accuracy and 0.100 top2-accuracy on *new measure* test. The ensemble model trained in *leave one battery out* experiment achieves 80% overall classification accuracy and 95% top2-accuracy on *new battery* SOC estimation test and 90% accuracy and 100% top2-accuracy on *new measure* test.

IV. CONCLUSIONS

Experimental results confirm that the relationship between EIS and SOC can be leveraged to estimate the SOC of a battery from impedance measurements. Although the analytical relationship is unknown, deep neural networks can be used as an approximated model to estimate SOC. We develop a SOC estimator based on CNN and a training pipeline that allows for fast system calibration on the specific battery to compensate for the variation in EIS present in each specific battery and the battery aging over time. The proposed system achieves 90% and 100% top-2-accuracy accuracy in SOC estimation for a battery included in the training. On an unknown battery the system scores a 62% accuracy and 80% top-2-accuracy.

REFERENCES

[1] Y. Chen, Y. Kang, Y. Zhao, L. Wang, J. Liu, Y. Li, Z. Liang, X. He, X. Li, N. Tavajohi, and B. Li, "A review of lithium-ion battery safety concerns: The issues, strategies, and testing standards," *Journal of Energy Chemistry*, vol. 59, pp. 83–99, 2021. doi:

10.1016/j.jechem.2020.10.017.

[2] E. Chemali, P. J. Kollmeyer, M. Preindl, and A. Emadi, "State-of-charge estimation of li-ion batteries using deep neural networks: A machine learning approach," *Journal of Power Sources*, vol. 400, pp. 242–255, 10 2018. doi: 10.1016/j.jpowsour.2018.06.104.

[3] C. Hu, L. Ma, S. Guo, G. Guo, and Z. Han, "Deep learning enabled state-of-charge estimation of lifepo4 batteries: A systematic validation on state-of-the-art charging protocols," *Energy*, vol. 246, p. 123404, 5 2022. doi: 10.1016/J.ENERGY.2022.123404.

[4] I. Babaeiyazdi, A. Rezaei-Zare, and S. Shokrzadeh, "State of charge prediction of ev li-ion batteries using eis: A machine learning approach," *Energy*, vol. 223, p. 120116, 2021. doi: 10.1016/j.energy.2021.120116.

[5] M. Galeotti, L. Cinà, C. Giammanco, S. Cordiner, and A. Di Carlo, "Performance analysis and soh (state of health) evaluation of lithium polymer batteries through electrochemical impedance spectroscopy," *Energy*, vol. 89, pp. 678–686, 2015. doi: 10.1016/j.energy.2015.05.148.

[6] K. J. M. C. J.-Y. Y. W.-S. Choi Woosung, Shin Heon-Cheol, "Modeling and applications of electrochemical impedance spectroscopy (eis) for lithium-ion batteries," *J. Electrochem. Sci. Technol*, vol. 11, no. 1, pp. 1–13, 2020. doi: 10.33961/jecst.2019.00528.

[7] M. A. Hannan, D. N. How, M. B. Mansor, M. S. H. Lipu, P. Ker, and K. Muttaqi, "State-of-charge estimation of li-ion battery using gated recurrent unit with one-cycle learning rate policy," *IEEE Transactions on Industry Applications*, vol. 57, pp. 2964–2971, 5 2021. doi: 10.1109/TIA.2021.3065194.

[8] K. He, X. Zhang, S. Ren, and J. Sun, "Deep residual learning for image recognition," in *Proceedings of the IEEE Computer Society Conference on Computer Vision and Pattern Recognition*, vol. 2016-December, 2016. doi: 10.1109/CVPR.2016.90.

[9] A. Guha and A. Patra, "Online estimation of the electrochemical impedance spectrum and remaining useful life of lithium-ion batteries," *IEEE Transactions on Instrumentation and Measurement*, vol. 67, 2018. doi: 10.1109/TIM.2018.2809138.

[10] I. Goodfellow, Y. Bengio, and A. Courville, *Deep Learning*. MIT Press, 2016. `http://www.deeplearningbook.org`.

[11] R. Pintelon and J. Schoukens, *System identification: a frequency domain approach*. John Wiley & Sons, 2012.

[12] A. D. Angelis, P. Carbone, A. Moschitta, M. Crescentini, R. Ramilli, and P. A. Traverso, "A fast and simple broadband eis measurement system for li-ion batteries," in *24th IMEKO TC4 International Symposium and 22nd International Workshop on ADC and DAC Modelling and Testing*, 2020. `https://www.imeko.org/publications/tc4-2020/IMEKO-TC4-2020-30.pdf`.

[13] A. De Angelis, E. Buchicchio, F. Santoni, A. Moschitta, and P. Carbone, "Uncertainty characterization of a practical system for broadband measurement of battery EIS," *IEEE Transactions on Instrumentation and Measurement*, vol. 71, pp. 1–9, 2022. doi: 10.1109/TIM.2022.3156994.

[14] E. Buchicchio, A. De Angelis, F. Santoni, and P. Carbone, "Data for: Dataset on broadband electrochemical impedance spectroscopy of lithium-ion batteries for different values of the state of charge." *Mendeley Data*, 2022. doi: 10.17632/ch3sydbbrg.3.

[15] E. Buchicchio, A. D. Angelis, F. Santoni, and P. Carbone, "Dataset on broadband electrochemical impedance spectroscopy of lithium-ion batteries for different values of the state of charge." *Mendeley Data*, 2022. doi: 10.17632/MBV3BX847G.3.

[16] J. Howard and S. Gugger, "FastAI: A layered API for deep learning," *Information (Switzerland)*, vol. 11, 2020. doi: 10.3390/info11020108.

[17] E. Buchicchio, "Machine learning for measurement: v0.2.0." *Zenodo*, June 2022. doi: 10.5281/zenodo.6484862.

[18] K. He, X. Zhang, S. Ren, and J. Sun, "Deep residual learning for image recognition," in *2016 IEEE Conference on Computer Vision and Pattern Recognition (CVPR)*, pp. 770–778, 2016. doi: 10.1109/CVPR.2016.90.

[19] L. N. Smith, "Cyclical learning rates for training neural networks," in *Proceedings - 2017 IEEE Winter Conference on Applications of Computer Vision, WACV 2017*, 2017. doi: 10.1109/WACV.2017.58.

[20] J. Howard and S. Ruder, "Universal language model fine-tuning for text classification," in *Proceedings of the 56th Annual Meeting of the Association for Computational Linguistics (Volume 1: Long Papers)*, (Melbourne, Australia), pp. 328–339, Association for Computational Linguistics, July 2018. doi: 10.18653/v1/P18-1031.

[21] B. Zhou, A. Khosla, A. Lapedriza, A. Oliva, and A. Torralba, "Learning deep features for discriminative localization," in *2016 IEEE Conference on Computer Vision and Pattern Recognition (CVPR)*, pp. 2921–2929, 2016. doi: 10.1109/CVPR.2016.319.

[22] F. Pedregosa, G. Varoquaux, A. Gramfort, V. Michel, B. Thirion, O. Grisel, M. Blondel, P. Prettenhofer, R. Weiss, V. Dubourg, J. Vanderplas, A. Passos, D. Cournapeau, M. Brucher, M. Perrot, and E. Duchesnay, "Scikit-learn: Machine learning in Python," *Journal of Machine Learning Research*, vol. 12, pp. 2825–2830, 2011.